Research article

High frequency ultrasound assesses transient changes in cartilage under osmotic loading

Jana Zatloukalova[1,2,3] **and Kay Raum**[2,*]

[1] Faculty of Nuclear Science and Physical Engineering, Czech Technical University in Prague, Břehová 7, 115 19 Prague, Czech Republic

[2] Charité–Universitätsmedizin Berlin, Corporate Member of Freie Universität Berlin, Humboldt-Universität zu Berlin, and Berlin Institute of Health, BCRT - Berlin Institute of Health Center for Regenerative Therapies, Berlin, Augustenburger Platz, 133 53 Berlin, Germany

[3] Institute of Thermomechanics, Czech Academy of Science, Dolejškova 1402/5, 182 00 Prague, Czech Republic

* **Correspondence:** Email: kay.raum@charite.de.

Abstract: High-frequency ultrasound is used in this study to measure noninvasively, by means of osmotic loading, changes in speed of sound and cartilage thickness caused by variations of the salt concentration in the external bath. Articular cartilage comprises three main structural components: Water, collagen fibrils and proteoglycan macromolecules carrying negative charges. The negatively charged groups of proteoglycans attract cations and water into tissue and govern its shrinkage/swelling behavior, which is a fundamental mechano-electrochemical function of cartilage tissue. In this study, the mechano-electrochemical behavior of cartilage is modeled by a diffusion model. The proposed model enables simulations of cartilage osmotic loading under various parameter settings and allows to quantify cartilage mechanical properties. This theoretical model is derived from the kinetic theory of diffusion. The objectives of the study are to quantify time dependent changes in cartilage thickness, and in speed of sound within tissue with help of the finite element based simulations and data from experiments. Experimental data are obtained from fresh and trypsinized ovine patella samples. Results show that the proposed diffusion model is capable to describe transient osmotic loading of cartilage. Mean values and their deviations of the relative changes of cartilage characteristics in response to chemical loading are presented.

Keywords: articular cartilage; high-frequency ultrasound; diffusion model; numerical simulations; osmotic loading; swelling behavior; fixed charge density

1. Introduction

1.1. State of the art—cartilage measurements

High frequency ultrasound is nowadays widely used in medicine as a noninvasive, irradiating, and affordable diagnostic tool. The dependence of speed of sound on the ion concentration in the propagation medium is used in this study to assess transient changes in thickness during articular cartilage swelling and shrinkage.

In early studies, the recovery swelling properties of articular cartilage (AC) were characterised by uniaxial confined compression through its dependence on external bath concentration [1–4]. The inhomogeneous recovery swelling was studied by cutting cartilage tissue into layers and testing them individually. Traditionally, the recovery swelling behavior of cartilage under osmotic loading was investigated by destructive approaches such as non-contact optical techniques [5, 6], or by confocal fluorescence scanning microscopy [7, 8] where the cross-sectioned images were analysed and features such as depth dependent recovery swelling were reported.

Later, the fixed charge density (FCD) was evaluated in a non-invasive way by a combined osmotic and mechanical loading approach and with help of theoretical analysis [9]. Lai et al. [10] introduced a triphasic mechano-electrochemical field theory for a charged, hydrated soft tissue. This continuum mixture theory applied to soft tissue, and combined with the physico-chemical theory represents a thermodynamic approach. By methods of mechanical loading the transient cartilage behavior has been modeled by Mow et al. [11].

In recent years, high-frequency ultrasound has increasingly been used for the assessment of mechanical cartilage properties. It provides a non-invasive way of monitoring transient changes of articular cartilage thickness and the detection of various acoustic parameters related to the biomechanical competence of AC in situ, such as speed of sound [12–16], and has been eventually combined with theoretical models [17, 18] to calculate additional mechanical parameters. Ultrasound approaches provide mechanical and morphological information nondestructively, and could be evaluated in a time-dependent and depth-dependent manner.

For example, 50 MHz ultrasound combined with an ultrasound palpator has been used [12] to measure mechanical properties of soft tissue layers in vitro in bovine samples. In the mentioned study, the thickness of the digested cartilage layer has been measured at various time points during trypsin digestion, and the equilibrium compressive modulus of the digested cartilage was found to be approximately ten times lower than that of the undigested sample.

Wang et al. [17] proposed a combined method, i.e., 50 MHz ultrasound is used first to study the depth-dependent strain magnitude of cartilage *in situ* under osmotic loading, and, secondly, the layered aggregate modulus of articular cartilage is determined using a triphasic model [10].

Also, ultrasound enables to monitor various loading techniques with minor influence on the loading procedure. Next to the traditional mechanical loading methods, and osmotic loading method used in this study, the method of dehydration has been used in [19] to study recovery behavior of normal and trypsin depleted cartilage samples.

In contrast to above mentioned studies, we use high-frequency ultrasound to measure the changes in cartilage thickness, both, during swelling and shrinking, and consider changes of the speed of sound within the tissue caused by changes in salinity of external bath solution. Also, we propose the diffusion model of osmotic loading and recovery swelling of articular cartilage using which the

cartilage mechanical properties can be quantified. This transient theoretical model is based on the kinetic theory of diffusion and considers fixed charge density. Experimental data are used in order to verify the model validity. Advantages of this approach are, e.g., the possibility to assess cartilage nondestructively and in real-time during shrinking and swelling phases of the experiment, the possibility to match experimental results to a theoretical model, and to simulate various model parameters settings (both, ultrasonic and morphologic), which may help to quantify the mechanical competence of the tissue.

1.2. State of the art—theoretical models of cartilage swelling

The confined compression stress relaxation tests have been frequently used for investigating the flow-dependent viscoelastic behavior of biological hydrated soft tissues [20]. From stress relaxation data, the 1-D compression modulus (i.e., aggregate modulus) at equilibrium can be well predicted by the poroelastic theory developed by Biot (1941) [21] or continuum mixture theory, i.e., the biphasic theory for cartilage developed by Mow et al. (1980) [20]. However, they do not account for the swelling pressure effect associated with the fixed charge density (FCD).

In contrary, the mechano-electrochemical theory [10] and [11] allows to study theoretically the swelling pressure effect associated with the FCD and, thereby, extend the both mentioned theories.

The former, called triphasic theory [10], is based on the continuum mixture theory of Truesdell and Noll [22] and Bowen [23], and combines the physico-chemical behavior [3, 24, 25], and the poroelastic or biphasic view [20, 21] in order to describe the deformational and flow behaviors of the tissue, and also accounts for the swelling pressure effect associated with the fixed charge density.

In triphasic theory, the driving forces for the movements of water and neutral salt in charged tissue are gradients of their chemical potentials, and depend on fluid pressure, salt concentration, solid matrix dilatation and fixed charge density. Stresses in the solid matrix are related to the Helmholtz energy functions in accordance with the laws of energy balance and entropy.

The later mentioned theoretical model accounts also for mechanical loading of tissue. The 1-D confined-compression stress-relaxation behavior of a charged hydrated soft tissue induced by a ramp displacement has been studied by Mow et al. [11]. The mathematical model is based on the continuum mixture theory developed for cartilage [10], and combined with a pair of coupled nonlinear partial differential equations governing the displacement of the solid matrix and concentration of the positive ions c_{Na}.

The triphasic theory [10] was applied on the problems of steady permeation flows generated by a hydraulic pressure difference [26]. There was shown that the water volume flux decreases nonlinearly with increasing FCD, thus also apparent permeability (associated with Darcy's law describing ability of a porous material to allow fluids to pass through it) decreases with increasing FCD. This was observed also by [3] and [27] where they showed the dependency of permeability on the compressive strain. For all of the pressure gradients tested the permeability of the cartilage decreased as the compressive strain increased.

Analogiclly to [26], the work of Gu [28] investigated the steady diffusion process through charged hydrated soft tissue under an osmotic pressure gradient. It was shown that in controlling the direction of osmotic flow (i.e. normal or negative osmosis) the major role plays the ratio of counter-ion diffusivity to co-ion diffusivity.

For negative osmosis to occur, the counter-ion diffusivity must be less than the co-ion diffusivity,

and then there is a critical value of FCD below which negative osmosis will take place, and above which the osmotic flow is ordinary.

Further generalization of the model as suggested, e.g., by Narmoneva et al. [6] can be achieved by depth-dependent distribution of FCD.

The diffusion model proposed in this work aims at describing the transient mechano-electrochemical behavior of cartilage under osmotic loading, i.e., its osmotic shrinking and recovery swelling. The advantages of the diffusion model compared to above described models are that it enables to model osmotic loading of intact cartilage sample, which is attached to the bone using parameters that might be gained from an ultrasonic experiment. An analogous experiment applied in vivo would allow to test mechanical loading noninvasively. Finally, using the diffusion model, healthy state of the cartilage might be inferred as the osmotic and mechanical loading are conditionally equvivalent [29].

1.3. Articular cartilage composition and function

Articular cartilage is a dense connective tissue of low friction that covers the surfaces of bones in synovial joints (e.g. knees, hips), and allows pain-free locomotion.

It consists of a sparsely distributed population of highly specialized chondrocyte cells that are embedded within a selfsynthesized macromolecular framework, as illustrated in Figure 1. Chondrocytes produce solid organic matrix of collagen, large aggregating proteoglycans, and specific noncollagenous proteins. Proteoglycans are composed of a protein core with attached negatively charged glycosaminoglycan chains. These structural macromolecules (approx. 20 to 40% of cartilage wet weight), together with tissue fluid (approx. up to 80% of the wet weight), form a strong cohesive porous hydrated extracellular matrix and give the tissue its stiffness, form, and resilience. The tissue is both aneural and avascular [30] and organized into a highly ordered structure. Extracellular matrix organization, composition, and cell morphology vary with depth from the articular surface. Four zones are commonly described [30], i.e., superficial, transitional, radial or deep, and the calcified cartilage zones (Figure 1).

In the superficial zone, flattened ellipsoid-shaped chondrocytes arrange themselves so that their major axes are parallel to the articular surface. There is a high concentration of collagen fibrils lying parallel to the joint surface, and a low proteoglycan concentration relative to the other cartilage zones.

In the transitional zone, cells become larger and more spheroidal in shape. Collagen fibrils have larger diameter and their long axes turn gradually towards oblique angles relative to the articular surface. The concentration of proteoglycans is higher.

The chondrocytes in the deep zone are spheroidal in shape and aligned in columns perpendicular to the joint surface. Collagen fibrils generally lie perpendicularly to the joint surface. The concentration of proteoglycans in this zone is the highest.

A thin calcified cartilage zone separates the deep zone and the subchondral bone.

Proteoglycan molecules (known as aggrecans) are composed of a single protein core to which glycosaminoglycan chains, usually chondroitin sulfate and keratan sulfate, are attached. At normal physiologic conditions, each dimeric unit of chondroitin sulfate has two negatively-charged groups (SO_3^- and COO^-), and each dimeric unit of keratan sulfate has one negative-charge group (SO_3^-). Thus, each aggrecan is a macromolecular polymer containing numerous negatively charged groups. Unlike the mobile ions (e.g., Na^+, Cl^-) dissolved in the interstitial water, these charges are firmly attached to the extracellular matrix, and thus they are called fixed charges. The density of these

charges is called the fixed charge density (FCD), and is usually reported in units mEq/g [31], which corresponds to 10^3 mol/m^3 in SI units, or also to mol/L NaCl.
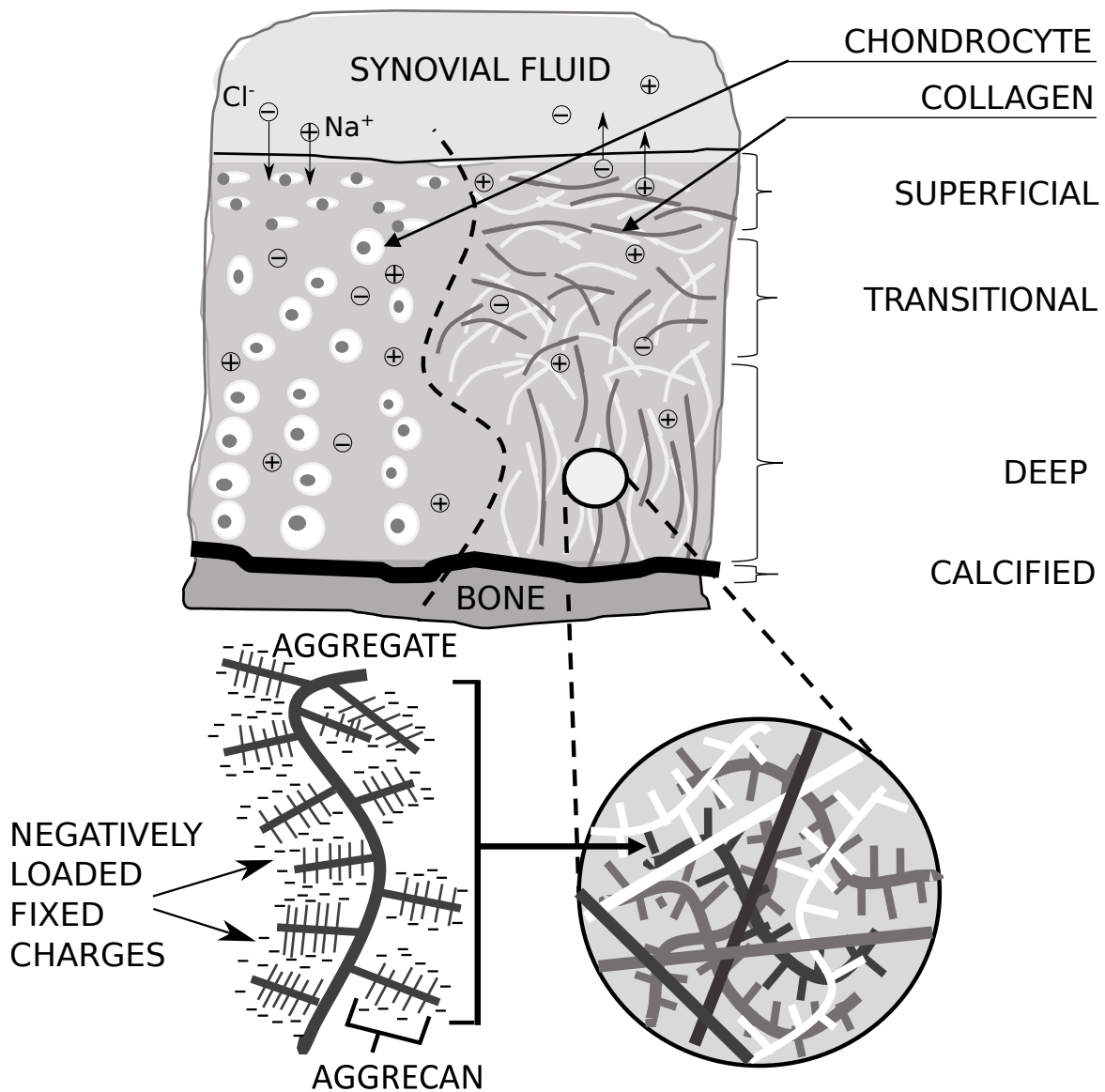

Figure 1. Schematic drawing of the zonal cellular (left) and collagen (right) architecture of articular cartilage. Chondrocyte cells are embedded in a solid collagen matrix, which maintains a dense suspension of large aggregates of aggrecan molecules with negatively loaded fixed charges attached, due to which cartilage is a negatively loaded tissue. Parallel to the surface, four zones can be distinguished, i.e., superficial, transitional, deep, and calcified cartilage zones. Between synovial fluid and cartilage tissue, positive and negative ions (Na^+, Cl^-) can move.

The negative fixed charges repel mobile anions (Cl^-), and attract mobile cations (Na^+) from the synovial fluid, and help keeping the fluid within the extracellular cartilage matrix. The concentration

of negatively-charged glycosaminoglycan chains varies with age and health state.

While the collagen fibrillar meshwork gives cartilage its form and tensile strength, the osmotic pressure caused by the mobile inorganic ions provide very good damping properties and high resistance against tensile stresses.

The tissue fluid contains a higher concentration of Na^+ (compared to Cl^-) to balance the negatively charged proteoglycans. Some fluid can move freely in and out of the tissue matrix, and this flow is generally accepted to be the pathway by which chondrocytes receive their nutrients and discharge their metabolic waste products [27]. However, it is also known that the diffusion of unbound molecules is enhanced by the cyclic compression and expansion during locomotion. During normal walking the forces across the cartilage surfaces vary from zero to more than three times the body weight [32].

1.4. Origin of the cartilage recovery swelling

Articular cartilage changes its volume, shape, and weight when the ion concentration in the external environment is changed [1]. This is referred to as chemical loading of cartilage.

Let us consider a cartilage sample immersed (at constant temperature) in physiological saline, which is a solution isotonic to body fluids. It contains 9.0 g of NaCl dissolved in one liter of sterile water, and corresponds to the concentration of 0.15 mol/L NaCl. If the salt concentrate in the surround fluid is increased, the tissue will shrink in an exponential manner. The smallest volume is reached at hypertonic concentrations as high as 2.5 mol/L NaCl [2]. A decrease of the ion concentration back to the physiological state causes cartilage to recover and to swell to its original dimensions. The amount of recovery swelling is constraint by the collagen fiber network. Under physiological conditions, cartilage is in a swollen state [10].

In addition to volume changes caused by ion concentration differences, the amplitude and kinetics of cartilage swelling and shrinking is governed by the number of negative fixed charges. The electrostatic interactions between fixed charges and mobile ions are primarily responsible for mechano-electrochemical coupling phenomena [1, 10].

Two conditions are fundamental for the tissue's swelling state—the electro-neutrality condition and the condition of minimization of concentration gradient.

The former requires that each fixed negative charge has a mobile counter-ion Na^+ in its vicinity to maintain electro-neutrality. In other words, the concentrations of mobile positive ions, e.g., Na^+, and mobile negative ions, e.g., Cl^-, and fixed negative charges fulfill the condition

$$c_{Na^+} = c_{Cl^-} + c_F, \tag{1.1}$$

whereas c_{Na^+}, c_{Cl^-} and c_F are the concentrations of the respective mobile ions and fixed charges.

The latter implies that mobile Na^+ and Cl^- ions diffuse between cartilage tissue and an external reservoir in order to reach equality of concentrations of mobile ions. However, for normal or hypotonic salt concentration, the total concentration of fixed and mobile charges within cartilage tissue is greater than in the reservoir, where no fixed charges are present. Consequently, molecules of H_2O flow into the cartilage in an attempt to equalize the ion concentrations on each side. This osmosis gives rise to a pressure in the interstitial tissue fluid being higher than the ambient pressure in the external reservoir, causing cartilage to swell. This is known as the Donnan osmotic pressure [25]. In the case of hypertonic salt concentrations, water molecules flow out of the cartilage tissue and

cartilage shrinks. This is described by the equation for equality of NaCl concentration c inside the soft tissue, and NaCl concentration c^* in the external solution [10]

$$(c^*)^2 = c(c + c_F). \tag{1.2}$$

Note, that in fluid $c^* = c_{Na^+} = c_{Cl^-}$.

The speed of sound is determined by salt concentration of propagating medium (other influences, such as temperature, etc., are held constant in our study). The salt concentration is quickly changed in external bath and, consequently, the salt concentration changes gradually also in cartilage tissue, causing speed of sound to increase gradually with higher salt concentration in tissue. Similarly, decrease in salt concentration causes decrease in speed of sound propagating through tissue. Note, that the overall tissue concentration is linked with fixed charge density.

High frequency ultrasound enables noninvasive and sensitive monitoring of transient changes in cartilage swelling and shrinking behavior, i.e., instantaneous changes in speed of sound and thickness of tissue under chemical loading, and, also, monitoring of the rate of these changes.

Chemical loading of cartilage tissue is equivalent to the usual mechanical loading of synovial joints caused by walking or running [29, 33]. During instant mechanical loading, the interstitial fluid bears all of the stress and exudes gradually through the cartilage surface into the synovial fluid. As the fluid is lost, the solid structure progresivelly deforms, transferring the load to elastic compression of the cartilage matrix. This corresponds to a change from physiologic to hypertonic ion concentration in case of chemical loading. Certainly, when the mechanical load is released, the cartilage re-imbibes fluid and swells due to the same principle as when the concentration is quickly changed back to the physiological state in case of chemical loading. Therefore, the osmotic loading can be used to determine the material properties characterizing cartilage function. However, it should be also emphasized that the speed of the loading in mechanical experiments can be chosen, whereas in chemical loading it is determined by the properties of the tissue.

Analogously to the in vitro thickness changes caused by chemical loading, the changes caused by mechanical loading, such as by walking or jumping, may be assessed in vivo by medical ultrasound.

According to [34], healthy cartilage does not expansively swell and its recovery swelling pressure is counteracted by considerable elastic forces within the collagen fibre network.

In contrary, degenerate cartilage easily expansively swells. Increase in water content and expansive swelling of articular cartilage is thought to result from fibrillation of the collagen network, which then becomes less able to restrain proteoglycan swelling forces, regardless of FCD dilution in the tissue due to degeneration [1].

In osteoarthritic degeneration of articular cartilage, damage can progress from fraying of localized collagen fibrillation of the superficial zone, followed by decrease in proteoglycan concentration, resulting in a complete erosion of the tissue layer covering the bone, leading to joint pain, restriction of motion, and even to a total joint disfunction. Risk factors for osteoarthritis development are, e.g., long-term mechanical overloading, but also immobilization and reduced loading which is insufficient for stimulation of protein synthesis [30]. Quantitative parameters of cartilage swelling behavior, e.g., relative change in cartilage thickness, and rate of shrinkage or swelling, may be useful for assessment of tissue mechanics and function, and can serve as an indicator of degenerative changes in the joint.

2. Materials and methods

2.1. Experimental setup

2.1.1. Articular cartilage specimens

Experiments were performed on four fresh patella samples of sheep aged between 2 and 4 years. Samples were visually classified as healthy with a smooth and intact surface. The specimens were taken from the body within one hour after sacrificing, were immersed immediately in physiological saline solution, stored at +4 °C, and measured within the next 12 hours. For the measurement of osmotic loading and recovery swelling, all changes reported hereinafter were defined as changes compared to the initial state measured in physiological saline at room temperature.

2.1.2. Ultrasound system and shrinking/swelling experiment

A medical ultrasound imaging system Ultrasonix Touch Research equipped with a high-frequency L40-8/12 linear array was used to monitor the transient swelling behavior noninvasively by transmitting focused ultrasound pulses into the tissue through the saline solution, and receiving the ultrasound echoes reflected from the cartilage surface and cartilage-bone interface Figure 2. Center frequency and -6-dB bandwidth were 12 MHz and 25%, respectively. Focus distance and depth of focus were 8 and 0.5 mm, respectively. The lateral scan field of the array was 12.8 mm. The container was filled with saline solution at 23 ± 0.5 °C, and the samples were fixed on the bottom of the container by silicone.
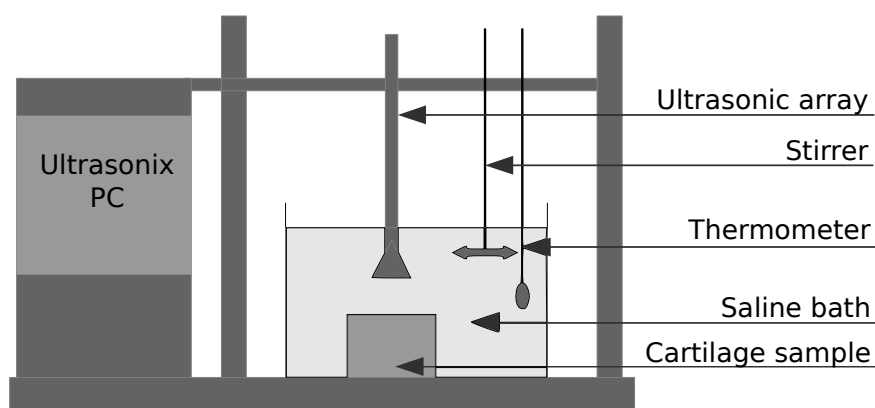

Figure 2. Experimental setup of the ultrasound swelling measurement system. The cartilage sample is fixed using silicone in the saline bath and centered beneath the ultrasonic array. During the experiment, the saline bath is well stirred and the temperature is recorded. The data are recorded and saved for postprocessing using a medical ultrasound imaging system (UltrasonixTouch).

The ultrasound transducer was fixed parallel to the specimen surface and centrally over the central part of the medial side of patella such that the focal zone was inside the AC tissue. The beamformed radio-frequency signals were recorded at a sampling rate of 40 MHz in time intervals of 3 s for 30 min.

The following initial configuration was set for particular samples. Before the experiment, each sample was left in normal saline solution at room temperature (23 ± 0.5 °C) for 30 min to equilibrate. During this time the transducer was positioned above the sample.

In the next step, the intrinsic shrinking/ recovery swelling experiment took place. Shrinking was induced by replacing the normal saline (0.15 mol/L) by a hyperosmolar (2 mol/L) solution. Consecutive ultrasound data were captured in time intervals of 3 s for 30 min. The first measurement was done within 30 s after replacement of the solution in the reservoir.

The temperature of the fluid was recorded throughout the experiment. A stirrer was used to maintain homogeneous distributions of temperature and ion concentration within the container during the experiments.

During recovery swelling phase, the bathing solution was changed in a short time from hypertonic concentration of 2 mol/L NaCl back to reference physiological concentration of 0.15 mol/L NaCl to observe the backward effect, i.e., the recovery swelling of the cartilage.

After shrinkage-swelling test the specimen was immersed in trypsin solution for approximately 12 hours, and stored at 4 °C. The trypsin solution depletes proteoglycans and mimics natural degeneration of the cartilage. After this procedure, shrinking and swelling after changing the ion concentration in the reservoir should be diminished because of the lack of fixed charges. However, diffusion should proceed anyway. To observe this, the shrinking-swelling test is performed on the treated samples again.

Figure 3 illustrates the ultrasound data collection and evaluation. Figure 3a depicts a single pulse-echo signal showing ultrasonic reflections from both, cartilage surface and the cartilage-bone interface. Figure 3b,c depict ultrasonic M-mode images, i.e., the time evolution of the pulse-echo signals. It can be seen that during the experiment the echoes reflected from cartilage surface and cartilage-bone interfaces gradually shift their pulse-echo travel times (Figure 3d) after saline concentration was changed from initial physiological concentration to hypertonic solution (as depicted in Figure 3b) and after 30 minutes back to physiological level (as depicted in Figure 3c).

2.1.3. Data processing

Based on the fact that the speed of sound depends on the salt concentration, temperature and pressure in the propagating medium, time dependent change of the salt concentration inside the cartilage is detectable from the reflection originating at the cartilage-bone interface, which shows apparent displacement. In fact, the cartilage-bone interface does not move when varying the surrounding salt concentration and the apparent displacement is caused by the change of time of flight (TOF) due to varying salt concentration. Temperature and pressure are kept constant. The displacements of the cartilage surface and apparent displacement of cartilage-bone interface were determined from the TOF of reflected ultrasonic echoes by tracking their shifts by peak-detection algorithm. First TOF after changing the medium was taken as reference. Experimental data were manually selected from the central part of the sample where the surface was even. For each sample, approximately 10 to 15 individual A-mode signals were processed individually and the results were averaged.
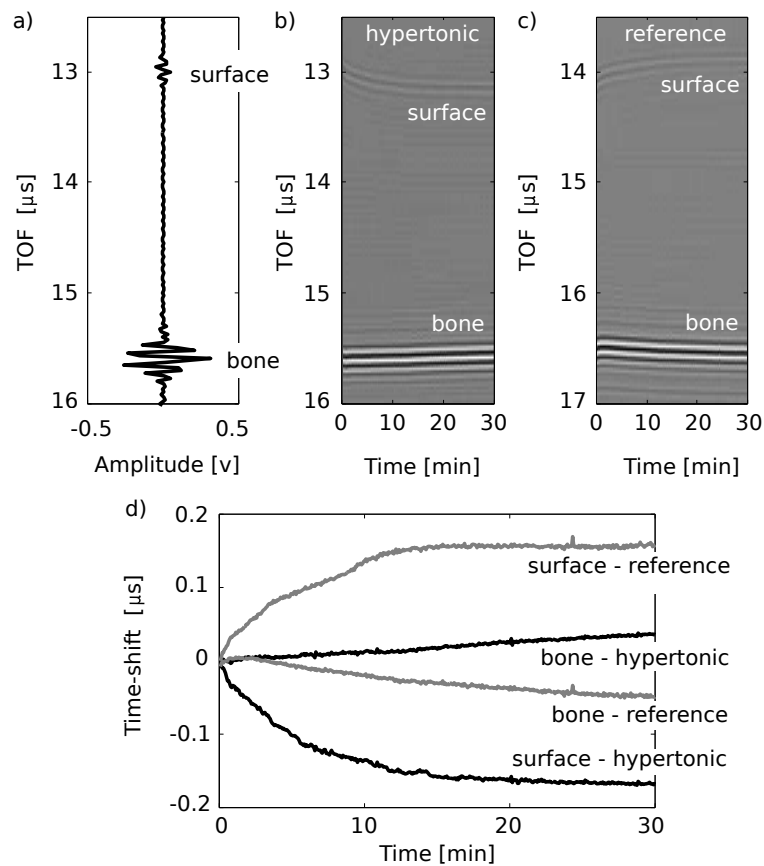
Figure 3. (a) A-mode showing time of flight (TOF) of ultrasound signal, which propagates from the transducer towards the cartilage sample, is reflected and travels back to the transducer where it is recorded. The upper peak of the signal corresponds to the reflection from cartilage surface, the lower peak corresponds to the reflection from cartilage-bone interface. Amplitude of the signal is displayed in grayscale in (b) and (c). The so-called M-mode images show pulse-echoes collected throughout the time duration of the experiment, (b) shows the transient osmotic loading phase and (c) the recovery swelling phase. Note that speed of sound changes with changing salt concentration in the external bath result in vertical axis shift of about 1 μs. (d) Time-shifts of the cartilage surface (surface-hypertonic) and cartilage-bone interface (bone-hypertonic) in the hypertonic bathing solution, and of the surface (surface-reference) and cartilage-bone interface (bone-reference) at the reference salt concentration are shown with respect to measurement time.

2.2. *Diffusion model*

Consider a one-dimensional ion diffusion problem along the x axis, see Figure 4a, of a specimen of charged hydrated soft tissue, e.g., articular cartilage, with thickness h, attached to the bone, and equilibrated in external bath solution of physiological concentration 0.15 mol/L NaCl. The concentration in external bath is assumed to be independent of time (i.e., the infinite reservoir condition). There is no externally applied mechanical pressure on the specimen, and temperature is kept constant.

After a quick change of external bath concentration to 2 mol/L NaCl, the cations (Na⁺) and anions (Cl⁻) diffuse from the high concentration side (external bath) to the low concentration side (cartilage tissue), i.e., in the negative x direction, and at the same time, water flows from the low concentration side to the high concentration side (ordinary osmosis). Consequently, cartilage specimen shrinks until it reaches an equilibrium.
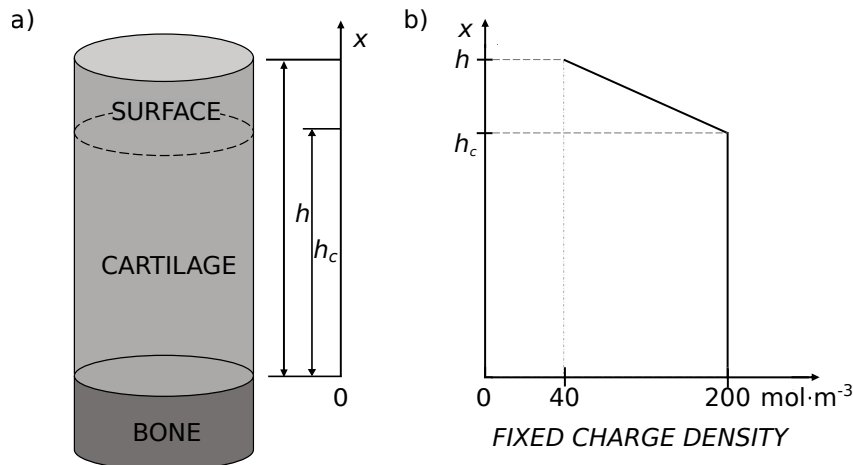

Figure 4. (a) Schematic diagram of the two-layered cartilage model with thickness of the whole cartilage layer h shown on the x axis, and (b) the distribution of fixed charge density within cartilage is gradually increasing in the surface zone $h - h_c$, and constant in the deep zone.

When the concentration of external bath solution is changed back to the physiological state, cartilage specimen recovers and swells to the original dimensions.

The change of dimensions, swelling or shrinking, depends on fixed charge density FCD c_F (i.e. density of the fixed charges attached to the extracellular matrix), the stiffness of collagen-proteoglycan matrix, and the ion concentrations in the interstitium.

Simulation of AC osmotic loading and recovery swelling characteristics requires the mathematical formulation of coupled mechano-electrochemical mechanisms between the AC and surrounding bath solution. We shall formulate this problem in terms of a system of four coupled partial differential equations for the ion concentrations (c_{Na^+}, c_{Cl^-}), for the electric field E, and for the extracellular matrix displacement e_x.

Following mathematical description couples the Nernst-Planck equation, the Poisson's equation and the mechanical deformation equation for one dimensional case. For this problem, all dependent variables are functions of the coordinate x and t only.

The Nernst–Planck equation describes the evolution of concentrations of chemical species in the fluid medium. It extends the Fick's law of diffusion to the case where the particles diffuse under the influence of both ionic concentration gradient and electrostatic forces:

$$\frac{\partial c_i(x,t)}{\partial t} = \frac{\partial}{\partial x}\left(D_i(x)\frac{\partial c_i(x,t)}{\partial x}\right) -$$
$$\frac{\partial}{\partial x}\left(D_i(x)\frac{z_i e}{k_B T}c_i(x,t)E(x,t)\right), \tag{2.1}$$

where t, D_i, c_i, z_i, e, k_B, T and E are, respectively, time, the diffusion coefficient of the i-th ion, the concentration of the i-th ion, valence of the i-th ion, elementary charge, the Boltzmann constant, temperature and electric field. In our case $i \in \{Na^+, Cl^-\}$.

In this equation, first term represents the diffusive flux due to the concentration gradient, the second term describes the migration flux due to the electric potential gradient. Both, diffusive flux and migration flux are driving forces which affect the motion of water and the individual mobile ionic species, Na^+ and Cl^-.

The second term is coupled with the equation for electric field:

$$\frac{dE(x,t)}{dx} = \frac{\rho(x,t)}{\varepsilon_0 \varepsilon_r}$$
$$= \frac{F}{\varepsilon_0 \varepsilon_r}\left(c_{Na^+}(x,t) - c_{Cl^-}(x,t) - c_F(x,t)\right), \tag{2.2}$$

where ρ, ε_0, ε_r, F and c_F are the charge density in the cartilage, the dielectric constant of the vacuum, the relative dielectric constant of the solvent, the Faraday constant and the FCD in the cartilage, respectively.

The cartilage shrinking and recovery swelling is described by the following equation for cartilage uniaxial deformation. Note, that the cases we study deal with the salt concentrations at the physiological level and higher. In these cases, cartilage is osmotically loaded and shrinks, or is unloaded and recovers until its initial state. Further expansive swelling due to hypotonic external bath concentration is not considered.

$$de_x(x,t) = -\frac{RT}{(\lambda_s + 2\mu_s)}\sum_{i \in \{Na^+, Cl^-, H_2O\}}\phi_i dc_i(x,t), \tag{2.3}$$

where e_x is the strain describing relative deformation with respect to the initial reference state given by physiological salt concentration, R is universal gas constant, T is temperature, and λ_s and μ_s are Lamé parameters for solid extracellular matrix. This equation relates the elastic stress in solid matrix due to deformation and the Donnan osmotic pressure, that depends on concentration differences of the fluid constituents, water and ions, integrated over the time-dependent thickness of the cartilage.

Here, the fluid is considered to be an incompressible mixture of three constituents: Water and the ion phase composed of two species: Na^+ and Cl^-. We denote by ϕ_i the volume fraction of each fluid component ($\phi_i = V_i/V$) fulfilling the condition

$$\sum_{i \in \{Na^+, Cl^-, H_2O\}}\phi_i = 1, \tag{2.4}$$

where Na^+ and Cl^- are assumed to be immiscible with the interstitial water and ϕ_{Na^+} and ϕ_{Cl^-} are very small (negligible) compared to ϕ_{H_2O}.

Calculation of water concentration c_{H_2O} has been done using the relation for the density of saline water v (in [cm^3/g]) which depends on temperature T (in [°C]), pressure P (in [bar]) and salinity S (in parts per thousand) [35]:

$$\{v(x,t)\}^* = 0.702+$$
$$\frac{100(a_1 + a_2\{T\} - a_3\{T\}^2 - a_4\{S\} - a_5\{T\}\{S\})}{\{P\} + b_1 + b_2\{T\} - b_3\{T\}^2 + b_4\{S\}}, \tag{2.5}$$

where salinity S depends on x and t, and where $a_1 = 17.527$, $a_2 = 0.110$, $a_3 = 0.0006$, $a_4 = a_4$, $a_5 = 0.0001$, $b_1 = 5880.9$, $b_2 = 37.592$, $b_3 = 0.34395$, $b_4 = 2.2524$, and for salinity holds

$$S(x,t) = (M_{Na^+}c_{Na^+}(x,t) + M_{Cl^-}c_{Cl^-}(x,t)) \cdot 0.001 \tag{2.6}$$

and where $M_{Na^+} = 22.99$ g/mol and $M_{Cl^-} = 35.453$ g/mol are molar masses of sodium and chlorine, respectively. Then, we calculated density of saline water ρ_s (in [g/m^3]), $\{\rho_s\} = \frac{1}{\{v\}}$, and using concentrations c_{Na^+}, c_{Cl^-} (in [mol/m^3]) of sodium and chlorine, and water molar mass $M_{H_2O} = 18.02$ g/mol, we can derive a formula for the concentration of water

$$c_{H_2O}(x,t) =$$
$$\frac{\rho_s(x,t) - (M_{Na^+}c_{Na^+}(x,t) + M_{Cl^-}c_{Cl^-}(x,t))}{M_{H_2O}}. \tag{2.7}$$

Equation (2.3) provides the values of relative deformation of the tested sample due to changes in concentrations during the experiment and gives theoretical description of the cartilage response on osmotic loading.

The apparent displacement of cartilage-bone interface depends on successive change of salt concentration in the cartilage tissue which causes changes in speed of ultrasound propagation within tissue. The information about the relative change in speed of sound SOS_{AC} is calculated by the relation

$$SOS_{AC}(t) =$$
$$k_{AC} \frac{\int_0^{x_c(t)} M_{Na^+}c_{Na^+}(x,t) + M_{Cl^-}c_{Cl^-}(x,t)\mathrm{d}x}{x_c(t)}$$
$$- k_{AC}(M_{Na^+}c_{Na^+_{min}} + M_{Cl^-}c_{Cl^-_{min}}) + v_{AC_{0.15M}}, \tag{2.8}$$

where $x_c(t)$ is the absolute thickness of the cartilage (calculated from Eq (2.3) and using initial value x_{c_0}, which was measured in reference state), and where

$$k_{AC} =$$
$$\frac{v_{AC_{2M}} - v_{AC_{0.15M}}}{(M_{Na^+}c_{Na^+_{max}} + M_{Cl^-}c_{Cl^-_{max}}) - (M_{Na^+}c_{Na^+_{min}} + M_{Cl^-}c_{Cl^-_{min}})} \tag{2.9}$$

The $v_{AC_{2M}} = 1750$ m s^{-1} and $v_{AC_{0.15M}} = 1670$ m s^{-1} are empirical values from [13], which are then adjusted to experimental results by fitting. Concentrations $c_{Na^+_{max}} = 2000$ mol/m^3, $c_{Cl^-_{max}} = 2000$ mol/m^3, $c_{Na^+_{min}} = 150$ mol/m^3 and $c_{Cl^-_{min}} = 150$ mol/m^3 were chosen according to the experimental procedure.

2.2.1. Initial conditions

In the initial state ($t = 0$), the charged hydrated tissue sample (Figure 4a) is equilibrated in external bath of physiological concentration $c^* = 150$ mol/m^3 NaCl in osmotic loading phase, or $c^* = 2000$ mol/m^3 NaCl in recovery swelling phase, and thus $\frac{\partial c_{Na^+}}{\partial t} = 0$ and $\frac{\partial c_{Cl^-}}{\partial t} = 0$. When equilibrated, the tissue with thickness h is in an initial configuration and its thickness does not change with time.

According to the relation (1.2) for salt concentrations inside the tissue and in external bath solution, it holds for concentration of cations Na$^+$

$$c_{Na^+}(x, 0) = [c_F(0) + \sqrt{c_F(0)^2 + 4c^{*2}(0)}]/2, \tag{2.10}$$

where $c_F(0)$ is the FCD at $t = 0$ (the initial swollen state).

For example, if the concentration in external bath is $c^* = 150$ mol/m^3 NaCl, and inside the tissue is a constant fixed charge density $c_F = 200$ mol/m^3 through the tissue depth, than the equilibrium concentration inside the tissue is $c_{Na^+} = 280$ mol/m^3 and $c_{Cl^-} = 80$ mol/m^3.

2.2.2. Boundary conditions

The bottom surface $x = 0$ (i.e., cartilage-bone interface) is assumed to be rigid, therefore,

$$e_x(0, t) = 0, \quad \text{at } x = 0. \tag{2.11}$$

Also, this boundary is assumed to be impermeable to water and ions, thus at this boundary

$$\frac{\partial c_{Na^+}}{\partial x} = \frac{\partial c_{Cl^-}}{\partial x} = \frac{\partial e_x}{\partial x} = 0. \tag{2.12}$$

At the upper boundary of the tissue $x = h$ (i.e., cartilage surface), the continuity of concentrations inside tissue and in external bath gives the conditions $c_{Na^+} = c^*$ and $c_{Cl^-} = c^*$ at the tissue—bath interface. It is also assumed that external bath solution is well stirred.

3. Results

3.1. Experiments

Before of the experiment with cartilage samples, the ultrasound measurement procedure was calibrated using a PMMA (polymethylmethacrylate) block to ensure the temporal stability of the experimental setup. The stirrer ensured uniform circulation of the saline in the bath and minimized temperature deviations caused by the environment or residual devices warming, and maximized a homogeneous ion distribution in the liquid. The temperature was continually measured during the experiment and stored for post processing. The maximal error in TOF caused by external non-osmotic influences was less than 0.01 μs, which corresponds to accuracies of SOS and thickness estimation $\pm$ 0.1 and $\pm$ 0.3%, respectively.

Relative change in cartilage thickness is depicted in Figure 5a in case of osmotic loading and in Figure 5b in case of recovery swelling. Corresponding relative changes of SOS derived from the reflection at the cartilage-bone interface are shown in Figure 5c,d. The apparent cartilage-bone

displacement results from succesive change in speed of sound within cartilage tissue due to salt concentration equilibration. Conversion between time of flight and speed of sound can be made using the relation

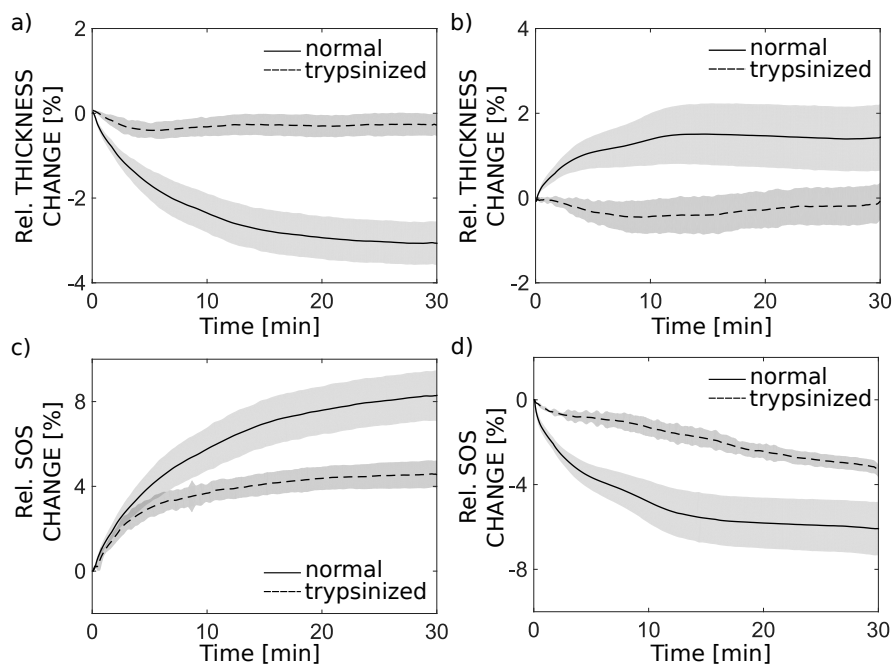$$\text{SOS}_{AC}(t) = \frac{2x_c(t)}{\text{TOF}(t)}.$$ (3.1)

Figure 5. (a) and (b) show relative change of cartilage thickness (surface displacement relative to cartilage thickness at the start of the experiment), and (c) and (d) show the relative change of speed of sound (SOS) within cartilage tissue. Ions propagating between external bath and cartilage tissue (in order to establish chemical equilibrium) cause a gradual change in speed of sound within the tissue. This gradual change can be detected by ultrasound as an apparent displacement of the cartilage-bone interface, because bone does not shrink or swell when changing the salt concentration. Note that temperature and pressure are held constant during experiment. The figures depict mean values and standard deviations from $N = 4$ samples during osmotic loading and recovery swelling for presumably healthy cartilage (thick line) and for trypsin depleted tissue (dashed line), respectively.

Mean values and their standard deviations of the relative thickness and speed of sound changes for $N = 4$ patella ovine samples are summarized in Table 1 for normal and trypsin depleted cartilage samples.

Table 1. Mean values and their standard deviations of the relative changes in cartilage thickness and speed of sound for $N = 4$ tested normal (N) and trypsinized (T) samples.

Relative change [%]	Shrinking	Swelling
Thickness (N)	-3.0 ± 0.4	+1.4 ± 0.8
Speed of sound (N)	+8.3 ± 1.2	-6.1 ± 1.2
Thickness (T)	-0.3 ± 0.2	-0.2 ± 0.4
Speed of sound (T)	+4.6 ± 1.6	-3.3 ± 0.3

3.2. Diffusion model

The coupled equations of diffusion models (2.1)–(2.3) and (2.8) subjected to the initial condition (2.10), and to the boundary conditions (2.11) and (2.12) are solved numerically using the finite difference method and the commercial software COMSOL Multiphysics. For articular cartilage, following empirical values and physiologically realistic initial parameters, taken from references [10, 36, 37], are used in our numerical study: $t_0 = 1800$ s, $x_{c_0} = 2.3 \times 10^{-3}$ mm, $R = 8.314$ J/(mol K), $T = 298$ K, $D_{\mathrm{Na}^+} = 5 \times 10^{-10}$ m^2 s^{-1}, $D_{\mathrm{Cl}^-} = 5 \times 10^{-10}$ m^2 s^{-1}, $c_F = 200$ mol m^{-3}, $H_A = (\lambda_s + 2\mu_s) = 30$ MPa, $\phi_{\mathrm{Na}^+}=0$, $\phi_{\mathrm{Cl}^-}=0$, $\phi_{\mathrm{H_2O}}=1$. The parameters were then adjusted by fitting in order to minimize the L^2-distance between the modeled curves and the data experimentally measured and averaged from $N = 4$ fresh ovine patella samples.

The following fits of parameters were used in numerical model for estimating variations in relative thickness and speed of sound, firstly in shrinking phase: $D_{\mathrm{Na}^+} = 9.5 \times 10^{-9}$ m^2 s^{-1}, $D_{\mathrm{Cl}^-} = 8.5 \times 10^{-9}$ m^2 s^{-1}, $H_A = 48.6$ MPa, $v_{\mathrm{AC_{2M}}} = 1843$ m s^{-1}, $v_{\mathrm{AC_{0.15M}}} = 1670$ m s^{-1}; and secondly in swelling phase: $D_{\mathrm{Na}^+} = 9.5 \times 10^{-9}$ m^2 s^{-1}, $D_{\mathrm{Cl}^-} = 8.5 \times 10^{-9}$ m^2 s^{-1}, $H_A = 32.4$ MPa, $v_{\mathrm{AC_{2M}}} = 1770$ m s^{-1}, $v_{\mathrm{AC_{0.15M}}} = 1628$ m s^{-1}. The RMSE values for variations of relative thickness and speed of sound are summarized in Table 2.

Table 2. RMSE values of the model curves for normal cartilage tissue. Note that the trypsin depleted samples are not evaluated because the model is inappropriate for cartilage with depleted fixed charges.

Relative change [%]	Shrinking	Swelling
Thickness	0.08	0.13
Speed of sound	0.05	0.25

4. Discussions

4.1. Relative change of cartilage thickness and speed of sound

In case of healthy cartilage, Zheng et al. [14] reported that the change from hyperosmotic solution back to physiological salt concentration of the external bath caused a smaller displacement of the sample surface than the change induced during the shrinking phase, and at the same time, the gradual change of the speed of sound in the sample due to propagation of salt into the tissue was comparable in both phases. These findings are in good agreement with our measurements.

Values in Table 1 show that in the case of normal cartilage, osmotic induced shrinking does cause a larger surface displacement than swelling and cartilage does not recover completely to its original thickness during the time of experiment.

The change of speed of sound in normal cartilage throughout the osmotic loading experiment has been reported to be 4.4 ± 2.1% in the shrinking phase and 5.6 ± 1.6% in the swelling phase [18]. In [16], changes in speed of sound were 5.2 ± 1.5% and 5.1 ± 1.1% in shrinking and swelling phases, respectively. Values for shrinking phase are slightly lower than in our experiment, whereas results of swelling phase are in a good agreement with both studies. A possible explanation of the deviation may be the type of cartilage used, i.e., bovine cartilage in cited studies versus ovine samples in our work.

On the other hand, in case of trypsin depleted cartilage samples, and similar as observed in our work, [14] reports no substantial shifts in cartilage thickness, while speed of sound in tissue changes due to diffusion of ions during both phases of the experiment. In [16], speed of sound change is reported as 5.1 ± 0.8% in shrinking phase and 4.9 ± 1.2%, which is in general agreement with the results in Table 1. Slightly lower values for swelling phase in our study as compared to [16] might be again caused by type of cartilage sample.

Further, the recovery swelling of normal cartilage attached to the subchondral bone was stated to be in the range of 6% over the concentration range 0–1.0 mol/L NaCl [2].

Similar results were observed in our study, see Table 1.

4.2. Osmotic loading and speed of sound in cartilage

The interrelationship of the speed of sound with cartilage composition, mechanical properties and degenerative state was tested on healthy and degenerated bovine knee samples [13]. It was shown that the speed of sound, in phosphate-buffered saline at room temperature 20 °C, decreases with progressing degeneration and gaining water content, and increases with proteoglycan and collagen content. Typical value for healthy cartilage was approximately 1680 m/s, for damaged cartilage 1560 m/s.

Transient depth-dependent osmotic swelling and solute diffusion in normal and degenerated fresh bovine patellae was studied by [14] using a focused beam of 50 MHz ultrasound (US). Healthy and trypsin depleted samples were bathed and monitored by US sequentially in solutins 0.15, 2 and 0.15 mol/L saline for 1 hour at room temperature 20 °C. In the measurements, the shift of the echo from the cartilage surface represents the thickness change of cartilage tissue caused by shrinking or swelling, and shift of the echo from the cartilage-bone interface represents the change of the US speed in the tissue induced by the diffusion of NaCl. The crucial assumption here is, that the temperature does not change during the whole experiment.

It was shown that normal bovine patella shrank during first several minutes and then almost recovered to its original state in approximately 1 hour when the solution was changed from 0.15 to 2 mol/L saline. Explanation of this phenomenon is reported as remaining unclear. However, the influences as, e.g., age and healthy fitness of the bovine or change in the speed of sound in water induced by the temperature variation due to replacement of the saline bath are not discussed, and may, in our opinion, contribute to the explanation of the observed feature.

Another explanation can offer the study of the osmotic loading of spherical gels [36] where the partial volume recovery was observed and modeled by the mixture theory [38]. This partial recovery behavior can be explained by passive transport mechanisms.

The partial volume recovery was observed also in our experiments with trypsin depleted cartilage

samples.

In recovery swelling phase [14], the displacement of the sample surface was reported to be very small when the saline solution was changed from 2 mol/L back to 0.15 mol/L for normal bovine cartilage.

In both experimental phases, upward and downward movements of the echoes of the US signals reflected from cartilage-bone interface suggested that salt penetrated gradually into and out of the tissue, respectively, causing successive changes in speed of sound in cartilage.

Further, proteoglycans were digested using trypsin enzyme and the experiment was repeated. During the measurement, the surface of the digested cartilage no longer substantially shifted, although the shift in the TOFs from the cartilage-bone interface indicated the change in speed of sound in tissue.

In our study, the Figure 5 and Table 1 show that for healthy cartilage, osmotic loading is reversible and the cartilage recovers almost completely to its initial thickness within 30 minutes. When the cartilage undergoes trypsin depletion, we do not observe swelling recovery within 30 minutes. This can be caused by the lack of the fixed negatively charged protheoglycans.

Interestingly, Wang [18] validated repeatability of the sequential change of salt concentration from physiological state 0.15 mol/L, to hypertonic concentration of 2 mol/L, and back to 0.15 mol/L measured by high-frequency ultrasound. Further, the average sound speed in cartilage was measured in 0.15 and 2 mol/L saline solution as 1675 ± 51 m/s and 1781 ± 48 m/s, respectively, at room temperature 20 ± 1 °C.

4.3. Expansive swelling and cartilage degeneration

Eisenberg and Grodzinsky [1] determined equilibrium constitutive relations for the chemical dependence of the cartilage total swelling stress. The model focuses on changes in the tissue swelling stress caused by changes in the ionic concentration of the external bath solution.

In very dilute hypotonic saline compared with physiological saline, normal cartilage will expansively swell only minimally, i.e., in the range of 1.5–3%, as reported by [1–4]. In other words, in normal articular cartilage the tendency of the proteoglycans to hydrate and swell is well constrained by the collagen network.

By contrast, osteoarthritic specimens usually swelled quite substantially. Even in those tissue samples in which there was only a very slight surface roughening, a considerable expansive swelling was observed [4]. Thus, increased hydration in osteoarthritic cartilage and its substantive expansive swelling is not related to a change in the quality of the proteoglycans, and that rather originates in an impairment of the collagen fiber network.

4.4. Diffusion model of cartilage swelling

Relatively low values of RMSE in Table 2 suggest that the proposed diffusion model is capable to reasonably well describe osmotic loading of articular cartilage. The advantage of the model lies in accounting for FCD (fixed charge density). The diffusion model provides explicit evolution equations for a depth-dependent modeling of cartilage tissue. Using this model, e.g., the extreme tissue overloading and time needed for recovery might be simulated which may help to protect cartilage against non reversible changes and damage of tissue.

On the other hand, using the diffusion model, the interpretation of real (possibly also in vivo measured) values from ultrasound measurements might enable better interpretation of cartilage behavior, possible weaknesses in cartilage structure or its composition, and thus more accurate diagnosis of possible starting cartilage degeneration.

4.5. Limitations

There are several factors which might cause deviations of the observed values from those reported in literature. Although efforts were made in order to keep consistency with known experimental conditions reported in the literature, not all the details were available, and not all conditions were possible to fulfill.

One of the obvious differences is the type of cartilage. In our study, fresh ovine samples from patella were used. On the other hand, in the cited literature, also bovine or porcine samples were investigated. Secondly, the basic experimental temperature may slightly change swelling properties of the samples, and, thus, measured values. In our study, we use room temperature of 23 ± 0.5 °C. In some studies, the room temperature of 20 ± 0.5 °C is used, e.g. [13] or [14]. Another reasons for slight deviations of experimental results are, e.g., site location on animal body of the harvested tissue samples, storage before the experiment (fresh versus frozen and afterwards thawed samples), or age of the animals.

The proposed diffusion model allows for the calculation of transient cartilage response to change in external-bath ion concentration, considers fixed charged density, and provides explicit evolution equations for cartilage parameters modeling with the possibility to set the various material properties in a depth-dependent way.

Although the diffusion model gives reasonable results for healthy cartilage samples, for modeling of swelling behavior in case of degenerated cartilage is inappropriate.

In healthy case, water is attracted into the charged tissue as follows from the electro-neutrality condition and from the equality of concentrations in the tissue and in external bath solution. When chemically loaded, cartilage shrinks mainly due to water outflow. Unloading leads to cartilage swelling due to water inflow. This is indicated by experiments: Healthy cartilage shrinks and swells in an exponential manner during the experiment.

However, only minor thickness changes were observed in case of trypsin depleted cartilage. The lack of proteoglycans prevents the tissue from swelling despite the changes in salt concentration. Equation (2.3) cannot be used anymore. A possible explanation is that the cartilage tissue after trypsin depletion is no more capable keeping the water (as, for example, a sponge) but it allows the water to flow freely from the inside out (as, for example, a spring mattress). Note that longer experimental measurement is required to ascertain that the equilibrium is reached.

5. Conclusions

In this paper, high-frequency ultrasound was used to monitor transient changes in thickness and speed of sound of articular cartilage caused by osmotic loading. Normal cartilage samples from ovine patella as well as trypsin depleted samples (simulating natural degeneration) were studied.

Also, the mathematical description of the osmotic loading and recovery swelling behavior of the articular cartilage in response to changes in external-bath ion concentration was presented. The numerical results were compared to experimental data. We paid attention to two cases: Normal

cartilage, and trypsin-depleted cartilage. Their shrinking/swelling properties differ mainly because of the presence of negative fixed charges. Based on estimated model parameters, material properties (e.g. speed of sound in cartilage tissue, change in tissue thickness under loading) can be inferred. In the outlook, the model still needs to be confronted with data from the histology.

Moreover, ultrasound allows in vivo investigation of joints of volunteers and patients. Due to its noninvasive, irradiating and relatively affordable manner, ultrasound may help to diagnose early degenerative changes in cartilage before they become irreversible. Our study suggests that changes in cartilage shrinking and recovery swelling behavior are associated with cartilage degeneration. Thus, they potentialy may be an ultrasound-detectable indicator of early degenerative changes in joints of patients.

Acknowledgments

Conflict of interest

The authors declare that there is no conflict of interest.

References

1. S. R. Eisenberg, A. J. Grodzinsky, Swelling of articular cartilage and other connective tissues: Electromechanochemical forces, *J. Orthop. Res.*, **3** (1985), 148–159.

2. V. C. Mow, J. M. Schoonbeck, Contribution of donnan osmotic pressure towards the biphasic compressive modulus of articular cartilage, *Trans. Orthop. Res. Soc.*, **9** (1984), 262.

3. A. Maroudas, Physicochemical properties of articular cartilage, *Adult Articular Cartilage*, (1979), 215–290.

4. A. Maroudas, J. Mizrahi, E. P. Katz, E. J. Wachte, M. Soudry, Physicochemical properties and functional behavior of normal and osteoarthritic human cartilage, *Articular Cartilage Biochem.*, (1986) 311–329.

5. D. A. Narmoneva, J. Y. Wang, L. A. Setton, Nonuniform swelling-induced residual strains in articular cartilage, *J. Biomech.*, **32** (1999), 401–408.

6. D. A. Narmoneva, J. Y. Wang, L. A. Setton, A noncontacting method for material property determination for articular cartilage from osmotic loading, *Biophy. J.*, **81** (2001), 3066–3076.

7. C. M. Flahiff, D. A. Narmoneva, J. L. Huebner, V. B. Kraus, F. Guilak, L. A. Setton, Osmotic loading to determine the intrinsic material properties of guinea pig knee cartilage, *J. Biomech.*, **35** (2002), 1285–1290.

8. C. M. Flahiff, V. B. Kraus, J. L. Huebner, L. A. Setton, Cartilage mechanics in the guinea pig model of osteoarthritis studied with an osmotic loading method, *Osteoarthritis Cartilage*, **12** (2004), 383–388.

9. C. C. B. Wang, X. E. Guo, D. Sun, V. C. Mow, G. A. Ateshian, C. T. Hung, The functional environment of chondrocytes within cartilage subjected to compressive loading: A theoretical and experimental approach, *Biorheology*, **39** (2002), 11–25.

10. W. M. Lai, J. S. Hou, V. C. Mow, A triphasic theory for the swelling and deformation behaviors of articular cartilage, *J. Biomech. Eng.*, **113** (1991), 245–258.

11. V. C. Mow, G. A. Ateshian, W. M. Lai, W. Y. Gu, Effects of fixed charges on the stress – relaxation behavior of hydrated soft tissues in a confined compression problem, *J. Solids Struct.*, **35** (1998), 4945–4962.

12. L. Qin, Y. Zheng, C. Leung, A. Mak, W. Choy, K. Chan, Ultrasound detection of trypsin-treated articular cartilage: its association with cartilaginous proteoglycans assessed by histological and biochemical methods, *J. Bone Miner. Metab.*, **20** (2002), 281–287.

13. J. Töyräs, M. S. Laasanen, S. Saarakkala, M. J. Lammi, J. Rieppo, J. Kurkijärvi, et al., Speed of sound in normal and degenerated bovine articular cartilage, *Ultrasound Med. Biol.*, **29** (2003) 447–454.

14. Y. P. Zheng, J. Shi, L. Qin, S. G. Patil, V. C. Mow, K. Y. Zhou, Dynamic depth–dependent osmotic swelling and solute diffusion in articular cartilage monitored using real–time ultrasound, *Ultrasound Med. Biol.*, **30** (2004), 841–849.

15. Y. P. Zheng, M. H. Lu, Q. Wang, Ultrasound elastomicroscopy using water jet and osmosis loading: Potentials for assessment for articular cartilage, *Ultrasonics*, **44** (2006), e203–e209.

16. Q. Wang, Y. P. Zheng, G. Leung, W. L. Lam, X. Guo, H. B. Lu, et al., Altered osmotic swelling behavior of proteoglycan-depleted bovine articular cartilage using high frequency ultrasound, *Phys. Med. Biol.*, **53** (2008), 2537–2552.

17. Q. Wang, Y. P. Zheng, H. J. Niu, A. F. T. Mak, Extraction of mechanical properties of articular cartilage from osmotic swelling behavior monitored using high frequency ultrasound, *J. Biomech. Eng.*, **129** (2007), 413–422.

18. Q. Wang, Y. P. Zheng, Non-contact evaluation of osmosis-induced shrinkage and swelling behavior of articular cartilage in situ using high-frequency ultrasound, *Instrum. Sci. Tech.*, **34** (2006), 317–334.

19. Q. Wang, Y. Y. Yang, H. J. Niu, W. J. Zhang, Q. J. Feng, W. F. Chen, An ultrasound study of altered hydration behaviour of proteoglycan-degraded articular cartilage, *BMC Musculoskeletal Disord.*, **14**:289 (2013), 1–7.

20. V. C. Mow, S. C. Kuei, W. M. Lai, C. G. Armstrong, Biphasic creep and stress relaxation of articular cartilage in compression: theory and experiments, *ASME J. Biomech. Eng.*, **102** (1980), 73–84.

21. M. A. Biot, General theory of three-dimensional consolidation, *J. Appl. Phys.*, **12** (1941), 155–164.

22. C. Truesdell, Thermodynamics of diffusion, in *Rational Thermodynamics*, Springer, New York, 1985.

23. R. M. Bowen, Incompressible porous media models by use of the theory of mixtures, *Int. J. Eng. Sci.*, **18** (1980), 1129–1148.

24. A. Maroudas, Biophysical chemistry of cartilaginous tissues with special reference to solute and fluid transport, *Biorheology*, **12** (1975), 233–248.

25. R. Chang, L. J. Kaplan, The donnan equilibrium and osmotic pressure, *J. Chem. Edu.*, **54** (1977), 218–219.

26. W. M. Lai, W. Y. Gu, V. C. Mow, Flows of electrolytes through charged hydrated biological tissue, *Appl. Mech. Rev.*, **47** (1994), 277–281.

27. J. M. Mansour, V. C. Mow, The permeability of articular cartilage under compressive strain and at high pressures, *J. Bone Jt. Surg.*, **58** (1976), 509–516.

28. W. Y. Gu, W. M. Lai, V. C. Mow, A triphasic analysis of negative osmotic flows through charged hydrated soft tissues, *J. Biomech.*, **30** (1997), 71–78.

29. W. M. Lai, W. Y. Gu, V. C. Mow, On the conditional equivalence of chemical loading and mechanical loading on articular cartilage, *J. Biomech.*, **31** (1998), 1181–1185.

30. J. A. Buckwalter, H. J. Mankin, A. J. Grodzinsky, Articular cartilage and osteoarthritis, *Instr. Course Lect.*, **54** (2005), 465–480.

31. *A Dictionary of Units of Measurement*, 2018. Available from: www.unc.edu/r̄owlett/units/index.html.

32. J. P. Paul, Loading on normal hip and knee joints replacement, in *Advances in Hip and Knee Joint Technology*, (eds. M. Schaldach and D. Hohmann), Springer-Verlag, Berlin, (1976), 53–77.

33. A. Maroudas, C. Bannon, Measurement of swelling pressure in cartilage and comparison with the osmotic pressure of constituent proteoglycans, *Biorheology*, **18** (1981), 619–632.

34. A. Maroudas, Balance between swelling pressure and collagen tension in normal and degenerate cartilage, *Nature*, **260** (1976), 808–809.

35. W. Wilson, D. Bradley, Specific volume of sea water as a function of temperature, pressure and salinity, *Deep-Sea Res.*, **15** (1968), 355–363.

36. A. Abazari, R. B. Thompson, J. A. W. Eliott, L. E. McGann, Transport phenomena in articular cartilage cryopreservation as predicted by the modified triphasic model and the effect on natural inhomogeneities, *Biophys. J.*, **102** (2012), 1284–1293.

37. S. G. Patil, Y. P. Zheng, J. Y. Wu, J. Shi, Measurement of depth-dependence and anisotropy of ultrasound speed of bovine articular cartilage in-vitro, *Ultrasound Med. Biol.*, **30** (2004), 953–963.

38. W. Y. Gu, W. M. Lai, V. C. Mow, A mixture theory for charged-hydrated soft tissues containing multi-electrolytes: Passive transport and swelling behaviors, *J. Biomech. Eng.*, **120** (1998), 169–180.